Antimicrobial Action and Clotting Time of Thin, Hydrated Poly(Vinyl Alcohol)/Cellulose Acetate Films Functionalized with LL37 for Prospective Wound-Healing Applications

Helena P. Felgueiras*, Marta A. Teixeira, Tânia D. Tavares, Natália C. Homem, Andrea Zille, M. Teresa P. Amorim

Centre for Textile Science and Technology (2C2T), Department of Textile Engineering, University of Minho, Campus de Azurém, 4800-058 Guimarães, Portugal

*Corresponding author:

Email: helena.felgueiras@2c2t.uminho.pt

Tel. +351 253 510 283

Fax: +351 253 510 293

Abstract. Poly(vinyl alcohol)/cellulose acetate (PVA/CA) films were prepared via a new method that combines principles from solvent casting and phase inversion. To guarantee some degree of flexibility, films were produced with a higher percentage of PVA compared to CA, from 90/10 to 50/50. The antimicrobial peptide (AMP) LL37 was then anchored using dopamine as a binding agent. Films were characterized in terms of functional groups, thermal stability, tensile strength, porosity, swelling and degradation (stability in physiological media at different pHs). The antimicrobial performance of LL37 surface-modified films was tested against *Staphylococcus aureus*, *Staphylococcus epidermidis* and *Escherichia coli* in dynamic environment and in the presence and absence of an albumin interface. LL37 treated films demonstrated great antibacterial efficacy against the three kinds of bacteria, ≈ 75% inhibition for *S. aureus*, ≈ 85% for *S. epidermidis* and ≈ 60% for *E. coli*, regardless of PVA/CA ratio. Presence of albumin reduced bacteria inhibition in all tested groups, most likely due to the binding of the protein molecules to the antimicrobial agents, reducing the free fraction available for bacterial killing. Films treated with LL37 accelerated clotting time (≈ 10 min) above vancomycin and bare surfaces, demonstrating great capacity to activate the intrinsic coagulation cascade.

Keywords: biodegradable films; peptide LL37; antibacterial action; accelerated clotting; wound-healing.

1. Introduction

Wound care is a growing industry that lately has been facing multiple challenges due to the increasing health care costs, aging of population, appearance of antibiotic-resistant pathogens, and rise in the incidence of diseases such as diabetes and obesity, known to difficult wound-healing.[1]

Unlike acute wounds which heal in a predictable amount of time following the stages of healing, coagulation, inflammation, proliferation and remodelling,[2] chronic wounds (CW) often fail to progress past the inflammatory phase. Subsequent to an injury, a blood clot (fibrin), serving as a temporary shield, protects the wounded tissue and induces degranulation of platelets. Neuthophils, inflammatory cells that act as first line of defense against pathogens, migrate towards the wounded site followed by macrophages and liberate potent proteolytic enzymes like elastase.[3, 4] In CW, the proteolytic activity is 10 to 40 times superior than in acute wounds, leading to a continuous degradation of endogenous and supplemental hormones, growth factors and proteins, extremely important for the injured tissue defense system and regeneration. These biochemical alterations disrupt the normal healing of the wounds, leaving CW with a defected cell matrix and debris impair healing, and without defenses against bacteria colonization, prolonged inflammation, and moisture imbalance.[1, 5, 6] An equilibrium between antimicrobial action and degradation effects is a common goal of many CW treatments. Currently, there is no treatment resorting to a single therapy effective enough for CW. Instead, a complex multistep approach is applied: nonviable tissues are removed by debridement; infection and inflammation are minimized with antibiotics/anti-inflammatory agents; moisture imbalance is corrected with an appropriate dressing; and epithelialization and granulation tissue formation is promoted via drug therapies.[2, 6, 7]

Bioactive dressings that incorporate drugs/antibiotics in their formulation have been suggested as an alternative to the set of conventional approaches described earlier.[8, 9] The use of topical antiseptics and antibiotics, including the alternative biological agents silver, povidone-iodine, chlorhexidine and polyhexamethylene biguanide, has been essential in to the treatment of CW, particularly in the fight against infections.[10] Since many of the microorganisms frequently found in CW are potentially pathogenic, infection control has been a requirement in CW dressing formulations. However, the rising of antibiotic-resistant pathogens has increased the need for more effective therapies. Antimicrobial peptides (AMPs) which act quickly against microbial cells by binding to the cytoplasmic membrane at different sites, disrupting it and

generating pores and/or by penetrating the membrane and interacting with various intracellular proteins simultaneously, reducing these microorganism's ability to develop resistance, have increased interest as a potential solution. AMPs display a broad spectrum of activity that is not inhibited by body fluids, wound exudates or biofilms, and are bactericide and not just bacteriostatic.[9, 11, 12] In the human body, cationic AMPs represent the first line of defense against many invading pathogens. The only known human cathelicidin, hCAP-18, is a major protein expressed constitutively within the neutrophils.[13] It possesses a highly conservative N-terminus cathelin domain that precedes the domain that encodes the antimicrobial peptide. hCAP-18 is stored as an inactive propeptide precursor that, upon stimulation, is processed into an active peptide, the LL37 (19.3 kDa).[14-16] LL37 has been shown to play a major role in the innate immune responses and inflammation, working as a potent chemoattractant for mast cells, monocytes, T lymphocytes and neutrophils, and thus contributing to the host defense against infections.[17] It displays a broad antimicrobial activity against both Gram-negative and Gram-positive bacteria, while maintaining a synergistic antibacterial effect with defensins. LL37 also promotes wound-healing, angiogenesis and arteriogenesis and acts as immune adjuvant.[6, 15, 17, 18]

In acute wounds, transcription of hCAP-18 into LL37 is up-regulated within a few hours. On the contrary, in CW there is a complete lack of translated protein, indicating that the mRNA is not properly translated or is being rapidly degraded.[19] In the present work, we propose to engineer a 3D film via solvent casting and phase-inversion from polyvinyl alcohol (PVA) and cellulose acetate (CA) blends, both widely used in wound-healing, and functionalized with LL37. The goal is to explore the potential of LL37 to inhibit microbial action and instigate clotting time when functionalized at the surface or within the matrix of PVA/CA films, for prospective CW treatments. With this approach, we intend to generate a new antimicrobial dressing that will combine the immunoregulatory/antimicrobial effects of the LL37, made inactive or degraded in CW, with the protective, flexible and breathable features of the polymeric film.

LL37 has been loaded onto nanoparticles or anchored onto a variety of materials for an improved antimicrobial action. For instance, LL37 has been grafted onto titanium surfaces via poly(ethylene glycol) spacer and demonstrated great capability to kill *Escherichia coli* (*E. coli*) on contact.[20] The same was observed when loaded onto poly lactic-co-glycolic acid (PLGA) nanoparticles[16] or functionalized onto electrospun poly(ethylene-oxide) nanofibers.[21] LL37 has also been combined with serpin A1 (a major physiological

elastase inhibitor and immunomodulator) and encapsulated onto solid-lipid nanoparticles made of glyceryl monostearate and α-L-phosphatidylcholine. Here, the synergistic activity of LL37 and serpin A1 enhanced the nanoparticles antibacterial activity against *Staphylococcus aureus* (*S. aureus*) and *E. coli* above the LL37 or serpin A1 alone.[22] More recently, LL37 was functionalized onto PVA/silk fibroin nanofibrous mats by solution blending, and revealed a great efficiency in killing skin bacteria, such as *Staphylococcus epidermidis* (*S. epidermidis*), and preventing biofilm formation.[23] To the authors knowledge, functionalization of LL37 has not yet been attempted on the surface of PVA/CA films for prospective applications in wound-healing. PVA is a water-soluble, biodegradable, non-toxic, biocompatible polymer with excellent physical and mechanical properties (i.e. swelling capacity, hydrophilicity and elasticity), low fouling potential and strong pH stability.[24] On its turn, CA is the acetate ester of cellulose, the most common natural-origin biopolymer on earth, endowed with unique nanostructure, remarkable physical-chemical properties (i.e. hydrophilicity), low cost and biocompatibility.[25] Combinations of PVA and CA are very common in filtration membranes, using CA as the main polymer for membrane backbone.[26] The combinations proposed in this study use inverse proportions, with PVA as backbone polymer, so flexible, thin, hydrated films can be manufactured.

As the antimicrobial mode of action of LL37 consists in the formation of pores and disruption of the microbial membrane, a physical binding agent that allows the AMP some degree of freedom, to act by contact or be released from the surface, was selected. Dopamine (DOPA) is a physical binding agent that possesses the ability to deposit via oxidative self-polymerization at slightly basic pH onto virtually any type and shape of surface.[27]

2. Materials and Methods

2.1 Production of PVA/CA Films. PVA (Mw 78,000, 88% hydrolyzed from Polysciences Europe GmbH) and CA (39.8 wt% acetyl content, Mw 30,000 from Sigma) were individually dissolved at 10 wt% in dimethylformamide (DMF, Fisher) for 6 h. To facilitate PVA dissolution in DMF the temperature was raised to 130 ºC. CA was dissolved at room temperature (RT) for the same period of time. Once completely dissolved, the temperature from the PVA solution was reduced to 60 ºC and the CA was combined, leaving the blend to homogenize for 2 h. PVA/CA films were prepared at the ratios 100/0, 90/10, 80/20, 70/30, 60/40, 50/50 and 0/100 v/v. In order to maintain a certain degree of flexibility in the resulting films, only high

percentages of PVA were tested. CA was used to increase the films porosity and, consequently, oxygen transfer. The 100 PVA and 100 CA, respectively PVA/CA 100/0 and 0/100 v/v, were used as control. 25 mL of each solution were casted onto clean glass petri dishes of 140 mm of diameter. After 15 min of resting (films reached RT), 50 mL of a clotting bath, composed of 8 wt% sodium sulfate (Sigma) and 4 wt% sodium hydroxide (Sigma),[28] were added and left in contact with the films for 24 h. This step is known as phase-inversion method. In the end, the films were washed several times in distilled water (dH_2O) to eliminate any trace of DMF or the clotting bath and maintained hydrated in dH_2O (exchanged twice a week) at 4 ºC before use (Figure 1). For characterization purposes, films were slowly dried for 5 days at 37 ºC before testing. This gradual dH_2O evaporation prevented any alteration to the film's structural integrity, mainly introduced by elevated temperatures.

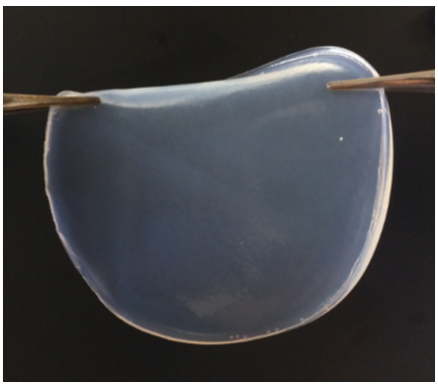

Figure 1. Aspect of the thin, hydrated PVA/CA films.

2.3 Attenuated Total Reflectance with Fourier-Transform Infrared Spectroscopy (ATR-FTIR). A Nicolet Avatar 360 FTIR spectrophotometer (Madison, USA) with an ATR accessory was used to record the PVA/CA films ATR-FTIR spectra. For each film, a total of 45 scans were performed at a spectral resolution of 4 cm^{-1}, over the range 400-4000 cm^{-1}.

2.4 Thermal Gravimetric Analysis (TGA). TGA measurements were conducted on a STA 449 F3 from NETZSCH Q500 using a platinum pan. The TGA trace was obtained in the range of 30-600 ºC under nitrogen atmosphere, flow rate of 20 mL/min and temperature rise of 10 ºC/min. Results were plotted as percentage of weight loss vs. temperature.

2.5 Differential Scanning Calorimeter (DSC) Analysis. DSC was carried out on a Power Compensation Diamond DSC (Perkin Elmer, USA) with an Intracooler ILP, based on the standards ISO 11357-1:1997, ISO 11357-2:1999 and ISO 11357-3:1999. Tests were conducted under a nitrogen atmosphere with a flow rate of 20 mL/min and heating rate of 10 ºC/min. The thermogram was obtained in the range of 30-500 °C. Results were plotted as heat flow vs. temperature.

2.6 Tensile Properties. The tensile strength and elongation at break of the PVA/CA films were evaluated using a Housfield H5KS dynamometer (Artilab) associated with the QMAT Materials Testing & Analysis software, following the standard ASTM D5035. Because of its fragile structural integrity (wet paper-like consistency), 100 CA films were not tested; only films containing PVA were tested. Three rectangular-shaped specimens of 8 cm long and 2 cm width were cut from each film. The average thickness of the samples was determined at approximately 0.08 cm. The gauge length and grip distance were established at 4 cm. The crosshead speed was 50 mm/min and the selected load cell was of 250 N, with a load range of 8 N and pre-load of 0.1 N. Experiments were conducted at RT.

2.6 Porosity and Degree of Swelling. The PVA-based films porosity was determined by measuring the mass loss after drying. Excess of dH_2O on the surface of the films was eliminated using kimwipes (Kimtech) prior to weighting. Films were weighted before and after drying for 5 days at 37 ºC, moment at which the films' mass reached a constant value. The porosity (ε) was calculated using the following equation:

(1) $\varepsilon = \frac{(m_w - m_d)}{AL\rho}$

where m_w (g) is the weight of the wet film, m_d (g) is the weight of the dry film, and A, L and ρ are the wet film effective area (cm^2), the wet film thickness (cm) and the dH_2O density (g/cm^3), respectively.

The films' degree of swelling (DS) was also determined by measuring the weight of the samples before and after drying. It was calculated using the following equation:

(2) $DS\ (\%) = \frac{(m_w - m_d)}{m_w} \times 100$

2.8 Degradation. Five solutions were used to test the degradation profile of the PVA/CA films over time: simulated body fluid (SBF) at pH 5 (average pH of intact skin), at pH 7.4 (physiological) and at pH 9 (average pH of chronic wounds), elastase buffer (from porcine pancreas, prepared at 45 mU/mL in 100 mM trizma hydrochloride or Tris-HCl at pH 8, Sigma) and commercial physiological serum (pH 5.8). In chronic, non-

healing wounds, the concentration of elastase in the wound fluid has been reported between 36 and 54 mU/mL.[29] Hydrated films of 1.1 cm in diameter and approximately 0.09 g in weight were incubated in 2 mL of each media at 37 ºC, up to 28 days. Experiments were conducted in static conditions, with media being exchange every week. After 1, 3, 7, 14, 21 and 28 days of incubation, the samples were weighted. Degradation, measured by mass loss, was calculated using the following equation:

(3) $Mass\ Loss\ (\%) = \frac{(m_{wi} - m_{wf})}{m_{wi}} \times 100$

where m_{wi} (g) is the weight of the hydrated film at day 0 (before sample immersion in each specific solution), m_{wf} (g) is the weight of the wet film after each time period.

2.9 LL37 and Vancomycin Functionalization. PVA/CA films of 1.1 cm diameter were functionalized with the AMP LL37 (Innovagen) and the antibiotic vancomycin hydrochloride (Sigma) using dopamine hydrochloride (DOPA, Sigma) as a binding agent. To prevent any contamination, films were initially sterilized with 70% ethanol (Merck) followed by washes with dH_2O. DOPA was prepared at 100 µg/mL in mM Tris-HCl at pH 8.5 and the sterile surfaces were immersed for 24 h at RT under 100 rpm (to prevent aggregates). For optimal polymerization conditions (conversion of DOPA into polydopamine or pDOPA), this step was conducted protected from light. pDOPA-coated films were then sonicated twice with Tris-HCl and once with dH_2O (2 min) to remove existing pDOPA precipitates, followed by several washes with dH_2O. The Minimum Inhibitory Concentration (MIC) of LL37 and vancomycin (non-functionalized) against *S. aureus*, *S. epidermidis,* and *E. coli* is always inferior to 50 µg/mL.[13] To prevent loss of action during functionalization, LL37 and vancomycin were prepared at 100 µg/mL in PBS. Films were immersed in each biomolecule solution for 12 h at 37 ºC, under static conditions. In the end, films were washed three times with PBS and unattached or weakly bound molecules were removed. The amount of vancomycin and LL37 functionalized was determined via amine groups detection using the sulfosuccinimidyl-4-o-(4,4-dimethoxytrityl)butyrate (sulfo-SDTB, Interchim). Briefly, 3 mg of sulfo-SDTB were dissolved in 1 mL of DMF and then adjusted to a final volume of 50 mL using a 50 mM sodium bicarbonate buffer (pH 8.5). Samples were immersed in a 2 mL solution containing 50% buffer and 50% working sulfo-SDTB solution and left to react for 40 min at RT and 150 rpm. Unbound reagent was eliminated by washing twice with dH_2O for 5 min using the orbital shaker. Immediately following the washes, hydrolysis of the adduct was induced with 2 mL of 1:1 methanol-

perchloric acid, which was left to react at RT and 150 rpm for 15 min. The concentration was determined by measuring the absorption intensity of the liberated dimethoxytrityl cation at 498 nm.

2.10 Antimicrobial Activity. The antibacterial efficacy of the LL37 and vancomycin functionalized PVA/CA films was assessed quantitatively following the standard ASTM-E2149-01, which determines the antimicrobial efficacy of an antimicrobial agent (functionalized or not) under dynamic conditions. Prior to the experiments, sterile films were pre-treated with bovine serum albumin (BSA, Sigma) at 4 mg/mL in phosphate buffer saline solution (PBS, pH 7.4) for 1 h. BSA has been shown to adsorb onto polymeric surfaces similarly to the human serum albumin (HSA); for that reason, BSA instead of HSA was used in the experiments.[27] The goal was to determine the influence of albumin, the most common protein present in the human blood plasma, on the efficiency of the functionalized LL37. Both Gram-positive and Gram-negative bacteria were used, respectively *S. aureus* (ATCC 6538) and *S. epidermidis* (ATCC 35984), and *E. coli* (ATCC 25922). The experiment was conducted aseptically to ensure the absence of any contamination. Bacteria inoculum were prepared from a single colony and incubated overnight in tryptic soy broth (TSB, Merck) at 37 ºC and 120 rpm. Each test was carried out using an initial concentration of 1.5-3.0 x 10^7 CFUs/mL in PBS. 1.1 cm diameter films weighting approximately 0.09 g were immersed in 2 mL of bacteria suspension and incubated at 37ºC and 100 rpm. After 0 h (before contact with sample) and 24 h of culture, the bacteria were serially diluted, cultured onto tryptic soy agar (TSA, Merck) plates, and further incubated for another 24 h. Quantitative results were obtained by counting the colonies of surviving bacteria on the agar plates. Antimicrobial activity was reported quantitatively in terms of % bacteria reduction calculated as the ratio between the number of surviving bacteria colonies present on the TSA plates, before and after contact with film. The death rate constant (mean $\log_{10}$ density) was only calculated for the LL37 and vancomycin in solution, since their % bacteria reduction was always superior to 90%.

2.11 Clotting Time. The clotting time of recalcified plasma in contact with the PVA/CA films was adapted from a procedure described previously.[30, 31] Briefly, 1.1 cm diameter sterile PVA/CA films, in the hydrated state, bare (control) and functionalized with LL37 and vancomycin were quickly dried with kimwipes. Tissue culture polystyrene (TCPS, Frilabo) was used as a negative control and glass slides (VWR) were used as positive control. A 1 M stock solution of calcium chloride ($CaCl_2$) was prepared and added to the recalcified

human plasma (citrated plasma, Sigma), thawed at 37 ºC, to obtain a final calcium concentration of 20 mM. The recalcified plasma was quickly mixed in a vortex, and 500 µL of the plasma solution were immediately added to each well containing the samples. The 24-well TCPS were incubated at 37 ºC and 150 rpm and the plasma clotting time was measured visually, as the time it took for the plasma to undergo gelation, detected by the loss of movement of the plasma in response to rotation and shaking.

2.12 Statistical Analysis. All experiments were conducted in triplicate. Numerical data were reported as mean ± standard deviation (SD). Statistical analysis was performed using ANOVA or Paired t-test, using the GraphPad Prism 7.0 software. Significance was defined as having $p<0.05$.

3. Results and Discussion

3.1 ATR-FTIR. Spectra of the PVA/CA films prepared at different ratios from 90/10 to 50/50, with 100/0 and 0/100 used as control, were collected (Figure 2). A wide adsorption peak between 3400 and 3200 cm^{-1} was observed on all films. It corresponded to the stretching vibrations of intermolecular hydrogen bonds of hydroxyl groups (-OH). It is also an indicative of the presence of moisture in the films that remained after the 5 days of drying at 37 ºC. Both PVA and CA have shown to bind strongly with water molecules.[32, 33] Because of the predominance of PVA in most mixtures, very little differences were observed between PVA and the combinations 90/10, 80/20, 70/30 and 60/40. It is however clear that some peaks characteristic of CA have appeared with the increased percentage of this polymer in the mixtures. Absorptions for anti-symmetric and symmetric stretching vibrations of $-CH_2$ in PVA occurred at approximately 2940 and 2900 cm^{-1}, respectively. In CA, a single adsorption peak was identified at 2900 cm^{-1} and corresponded to the stretching vibrations of the -CH of methyl groups ($-CH_3$).[34, 35] At 1740 cm^{-1}, the first difference in the PVA/CA films compared to 100 PVA is observed; this was most noticeable when the CA content was superior to 10%. This peak is assigned to the carbonyl (C=O) stretching vibrations and is characteristic of the CA acetyl groups, thus confirming the presence of CA within the mixtures. In anhydrous CA, this band is usually located at 1752 cm^{-1}, rather than 1740 cm^{-1}, and was found to shift towards longer wavelengths and to decrease in intensity upon hydration of its ester carbonyl groups.[32, 36] Once again, we realize the intimate bond that is generated between CA and water molecules. In a parallel experiment, spectra of samples dried at 60 ºC for 5 days were collected and evaluated; here too, the C=O stretching vibrations peak was identified at 1740 cm^{-1} (data not shown) and,

thus, demonstrating the difficulty in eliminating water from the film. The peak at 1650 cm^{-1} is associated to -OH deformation vibrations. The absorption peaks at 1420 and 1090 cm^{-1} are attributed to the $-CH_2$ bending and -C-O stretching of PVA groups, respectively.[37] The peaks at 1330 and 850 cm^{-1} are also attributed to PVA, namely to the $-CH_2$ bending vibrations. Finally, a small peak at 1143 cm^{-1} may be attributed to the stretching vibration of -C-C-C and -C-O bonds, which intensity is related to the crystalline structure of PVA.[38, 39] Interestingly, a small peak located at 1370 cm^{-1}, and not found in PVA, was detected in all mixtures. This is associated with the -C-H symmetric deformation vibration of the acetate group in CA. At 1240 cm^{-1} it is possible to identify the characteristic peak of -C-O-C related to the anti-symmetric stretching vibrations of the CA ester group.[40] The band between 1090 and 1000 cm^{-1} is associated with the stretching modes of -C-O single bonds, while the absorption peak at 904 cm^{-1} may be due to the combination of the -C-O stretching with the $-CH_2$ rocking vibrations.[34] The intensity of some of these peaks became more important as the content of CA in the films increased. However, because of the overlapping of bands between CA and PVA, analogous spectra predominated, and only little differences were observed.

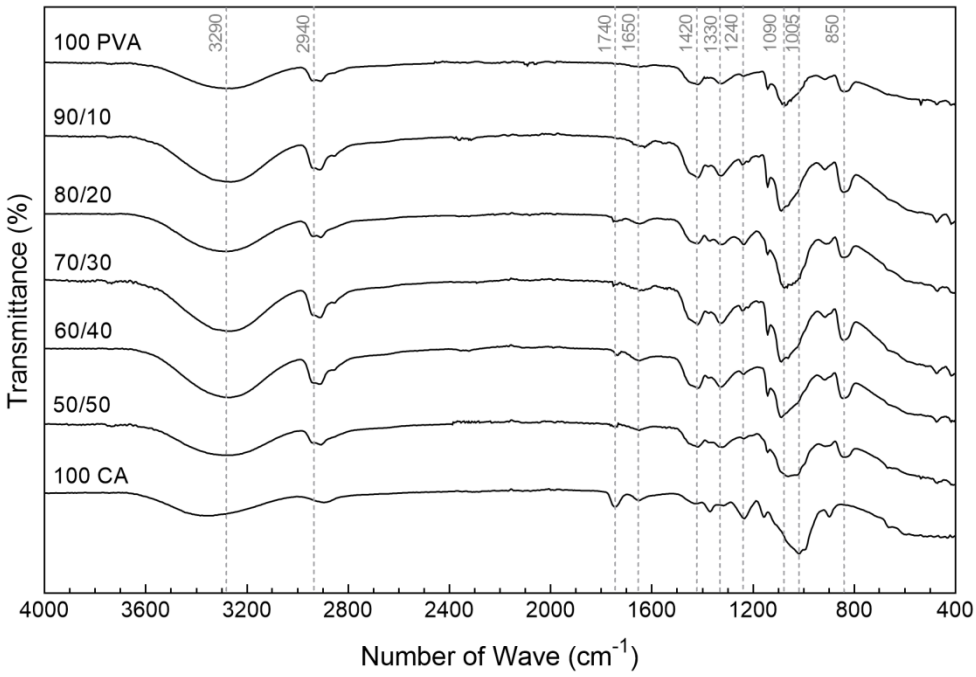

Figure 2. ATR-FTIR spectra of the PVA/CA films (4000-400 cm^{-1}).

3.2 TGA. Degradation steps associated with temperature rising were recognized on the PVA/CA films via TGA (Figure 3). The first step of degradation was identified between 30 and 75 ºC for 100 CA and between 30 and 150 ºC for 100 PVA (Table 1). As the content of PVA is more important than CA in most mixtures, the last temperature range (30-150 ºC) was observed for the remaining PVA/CA films. It refers to the initial volatilization of moisture, and possible remaining residues of solvent (DMF), from the specimens due to evaporation or dehydration of hydrated cations.[41] Because the first degradation event for PVA reaches temperatures above 100 ºC, it is possible that remaining molecules of DMF to act as plasticizers, as consequence of the initial degradation of the sections of polymer chains that interacted with the solvent via hydrogen bonding and, as such, being more difficult to eliminate.[37] Usually, PVA is characterized by only two degradation steps. Here, however, three were identified. The second degradation step was detected at 232 ºC (Table 1) and was attributed to the cleavage of the PVA polymeric backbone, which initiates with the degradation of the side chains and progresses to the main chain scission (355 ºC), until only carbon char remains (6.15% of residual mass at 600 ºC, Table 1).[42] In case of 100 CA, the second degradation step was detected at approximately 220 ºC, while the third was found at almost 340 ºC. Here, the CA polymeric chains undergo depolymerization, as the absorbed energy activates the cleavage of the glycosidic linkages producing glucose, which is then dehydrated in levoglucosan and oligosaccharides. The progression from the second to the third degradation steps is very smooth and gradual, during which the production of volatile compounds is complete (≈ 380 ºC, with almost 80% mass loss).[43, 44] After this temperature, the continuing weight loss is ascribed to further degradation into carbon char (14.29% of residual mass at 600 ºC, Table 1).

All mixtures of PVA and CA, from 90/10 to 50/50, were characterized by three degradation steps, which initial temperatures were found in between the degradation points of 100 PVA and 100 CA. Generally, it was seen that the degradation temperatures decreased with the increased content of CA; this is to be expected since the three degradation steps of CA were detected 70, 10 and 20 ºC earlier than those of PVA (in order). Small shifts in this progression may be related with the possible inter- and intra-molecular bonds generated between the two polymers. Interestingly, the second degradation peak for all mixtures did not follow the progression of neither 100 PVA nor 100 CA. The CA reinforcement was able to increase the thermal stability of the PVA, altering the thermogravimetric profile of the films. These findings are consistent with previous reports.[44] Indeed, the pattern of degradation becomes more important only at the third step, even though the second

represents already ≈ 20% of mass loss for both 100 PVA and 100 CA (compared to the ≈ 5% for the polymeric blends). Because of important internal rearrangements and intermolecular bonds (hydrogen bonding) generated between the polymers, the mixtures were able to maintain their integrity for longer, undergoing little degradation at temperatures below 340 ºC. Overall, the residual mass at 600 ºC was found similar between mixtures, varying only 3 ºC (Table 1), and, as expected because of CA presence, was slightly superior to that the 100 PVA.

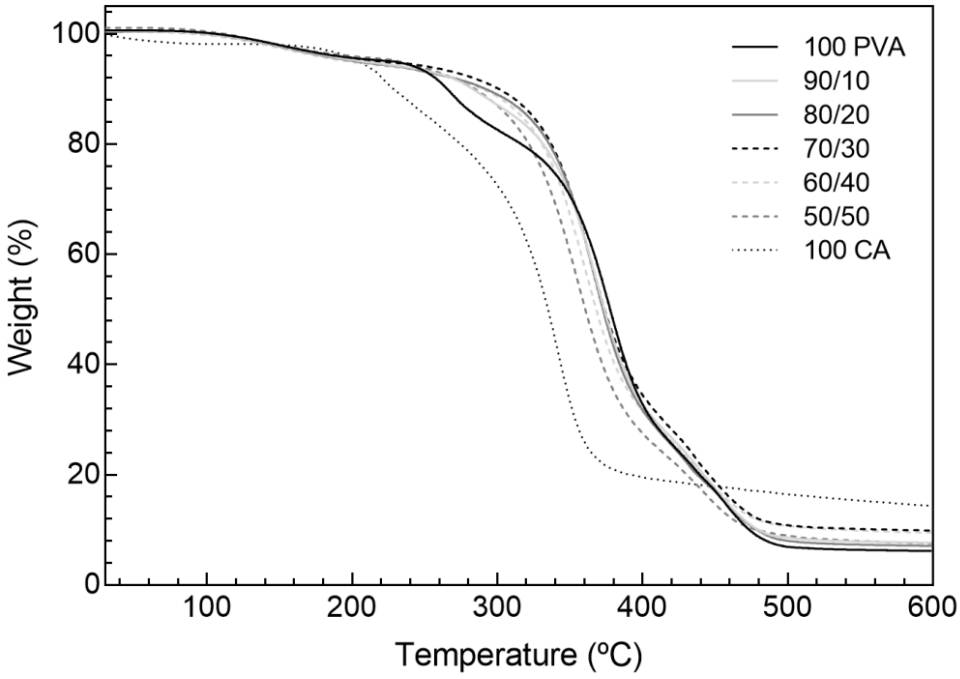

Figure 3. TGA of the PVA/CA films from 30 to 600 ºC, performed at a heating rate of 10 ºC min^{-1} in a nitrogen atmosphere.

3.3 DSC. DSC technique measures the physical and chemical transformations the PVA/CA films undergo when subjected to heating. DSC thermograms of the PVA/CA films prepared at different ratios were acquired between 30 and 500 ºC (Figure 4). For most of the films, the first endothermic peak was detected at a temperature ranging from 140 to 155 ºC; the only exception was 100 CA, which first peak was detected at 78.30 ºC (Table 1). The endothermic peak shifts to higher temperature regions as the content of CA in the film reduces. These peaks are known as dehydration peaks and occur due to the evaporation of water molecules

bonded to the hydrophilic groups of the polymers.[42, 45] The second peak was attributed to the melting temperature (T_m) of the polymeric film. Here, no T_m was observed for 100 CA since the polymer starts degrading prior to melting (≈ 220 ºC).[44] The average endothermic energy was seen to decrease as the amount of CA in the film increased. These results are consistent with previous findings[37] and suggest a good interaction between both polymers probably through hydrogen bonding via their respective hydroxyl groups. At temperatures around 360 ºC another endotherm peak is detected for most films. This is associated with the cleavage and degradation of the main backbone chains of PVA. For CA, this endotherm is registered at 345.67 ºC and is also associated with weight loss, as observed by TGA, namely the degradation of polymer main chains.[46] The last endotherm peak registered for the PVA-based films was detected around 430 and 440 ºC (Table 1) and was attributed to the final degradation of the remaining residual polymeric chains into carbon char. This peak was more important as the content of PVA increased.

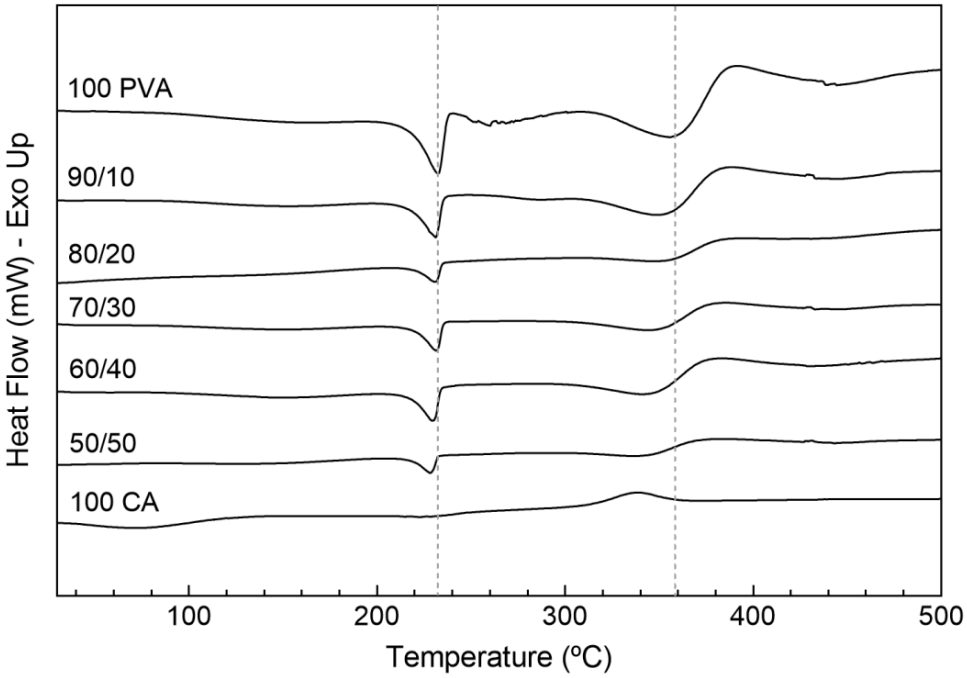

Figure 4. DSC thermograms of the PVA/CA films in a temperature range from 30 to 500 ºC, performed at a heating rate of 10 ºC min^{-1} in a nitrogen atmosphere.

Table 1. Main DSC thermal transitions, TGA weight loss temperature peaks and residual weight (n=3; S.D.<1%).

Films	Tm (ºC)	ΔH (J g^{-1})	T peaks of 1st derivative (°C)	Residue at 600 ºC (%)
100 PVA	150.60; 231.89; 355.36	23.42; 91.42; 231.95	156.65; 376.94; 435.41	6.15
90/10	148.66; 230.53; 349.77	38.89; 83.79; 229.92	154.13; 368.64; 431.34	7.66
80/20	148.10; 230.80; 352.66	32.69; 75.86; 200.86	152.76; 365.96; 430.83	7.09
70/30	147.06; 231.03; 344.67	53.43; 77.14; 226.05	148.63; 365.58; 439.45	9.86
60/40	146.43; 229.24; 343.50	44.68; 65.35; 196.98	150.26; 359.49; 438.17	9.45
50/50	140.95; 229.06; 341.52	65.00; 60.94; 157.68	140.76; 355.02; 443.54	7.48
100 CA	75.98; 222.23; 337.73	101.00; 35.53; 84.55	78.30; 220.02; 345.67	14.29

3.4 Tensile Properties, Porosity and Degree of Swelling. The breaking strength and elongation at break were determined for each PVA/CA film produced (Table 2). Rectangular shaped samples of 8 cm long, 2 cm width and 0.08 cm thickness were used. CA is a brittle polymer which exhibits notably high Young's modulus and a very small elongation at break.[47] Here, because of the mashed paper-like consistency, 100 CA films could not be explored in terms of mechanical performance. However, by combining PVA with CA, interactions were generated between free hydroxyl groups present in both polymers (hydrogen bonding), increasing the flexibility of the cellulose derivative chains and decreasing the films' fragility. Even though the mechanical stability of CA improved when combined with PVA, the films breaking strength and elongation at break reduced with the increasing content of CA in the blend. These results demonstrate that the mechanical properties of the films are governed by the natural polymer, as the weakest material in the blend. The porosity is also an important factor affecting the mechanical strength of a film. Here, once again, the content of CA plays an important role in defining the porous structure of the film; the porosity was more important as the percentage of CA in the blend increased. As such, the films became less compact and more susceptible to break under loading. Fluid uptake is an important parameter in wound-healing that influences the chemical and physical characteristics of the films, thus conditioning blood components interaction and exudates absorbency. The degree of swelling of the films was determined by measuring variations in weight after 5 days immersion in dH_2O at 37 ºC. Data from Table 2 does not show a proportional variation as mechanical testing and porosity determinations did with CA content. In fact, it appears that both low contents and high

contents of CA to increase water uptake. Even though there are no significant differences between films, the small reduction experienced by 80/20 and 70/30 blends may reflect more inter- and intra-polymer reactions, which may have reduced the number of hydrophilic groups available, thus contributing to a slightly more hydrophobic network.[48] It has been shown that water absorption alters the polymeric chains distribution and bonding opportunities, weakening the hydrated films' mechanical resistance.[49] These results explain the small breaking strengths registered for all PVA/CA blends, which are not proportional to the water uptake, thus reflecting the importance of hydrogen bonding between polymers and between polymeric chains and water molecules.

Table 2. PVA/CA films breaking strength (N) and elongation at break (%) determined while hydrated, and porosity (%) and degree of swelling (%).

Films	**Breaking Strength (N ± SD)**	**Elongation at Break (% ± SD)**	**Porosity (% ± SD)**	**Degree of Swelling (% ± SD)**
100 PVA	3.24 ± 0.03	253.53 ± 26.99	29.07 ± 5.12	89.87 ± 0.95
90/10	2.56 ± 0.14	247.00 ± 47.27	30.90 ± 2.43	89.26 ± 0.47
80/20	2.52 ± 0.25	244.47 ± 23.26	33.40 ± 3.79	88.35 ± 0.85
70/30	1.49 ± 0.18	244.20 ± 39.78	37.52 ± 6.81	88.12 ± 0.79
60/40	1.48 ± 0.15	222.13 ± 48.87	44.92 ± 2.15	89.01 ± 0.56
50/50	1.28 ± 0.20	201.87 ± 41.17	52.99 ± 4.95	89.21 ± 1.15
100 CA	-	-	91.83 ± 14.62	89.62 ± 1.00

3.5 Degradation. The stability of the PVA/CA films was evaluated in five physiological media: SBF at pH 5 (average pH of intact skin), at pH 7.4 (physiological) and at pH 9 (average pH of chronic wounds), elastase buffer at pH 8, and commercial physiological serum at pH 5.8. SBF solutions have osmolarity and ion concentrations that match those found in the human body, particularly blood plasma. Elastase is a potent proteolytic enzyme which activity increases 10 to 40 times in CW, leading to a continuous degradation of endogenous and supplemental hormones, growth factors and proteins, and ultimately preventing tissue regeneration.[3, 4] Variations in pH and presence of proteolytic enzymes may compromise the integrity of the dressing during wound-healing. As such, variations in the films mass were monitored up to 28 days of incubation at 37 ºC (Figure 5). Additionally, PVA/CA films were incubated in commercial physiological

serum in order to determine their stability with time while in storage. Data revealed, that most films lost over 20% of their initial mass after 28 days of incubation. The pH of the SBF solutions impacted on the degradation profile of the films. The most acidic solution registered slightly superior mass loss, quickly followed by the most basic; however, differences were not significant. In the presence of oxygen, water decomposes in OH^- and H^+ radicals. This phenomenon is increased at low and high pHs, leading the radicals to participate in oxidation reactions of the polymer macroradicals and, thereby, making chemical effects dominant in the degradation of the PVA/CA films. The acidic media (SBF at pH 5) increased the H^+ catalysis effect, accelerating hydrolysis of the ester groups in the polymers and, consequently, initiated the bulk degradation mechanism.[50] At pH 9, however, this process was not as quick, since carbon oxides, formed from the degradation of PVA, give rise to bicarbonate and carbonate ions under alkaline conditions, which may hinder degradation of the PVA/CA films,[51] hence explaining the small variations in mass between the two solutions. Interestingly, films with the most content of CA (with 100 CA included) experienced an increase in mass in the first days of incubation. SBF is a physiological solution with an ion concentration close to that of human blood plasma; as such, it is majorly composed of sodium, potassium, magnesium, chloride and bicarbonate ions. It is likely that, because of their larger surface area (increased porosity), the free hydroxyl groups in the films with the highest content of CA were more accessible to the ions in solution, thus sharing more interactions and increasing the overall mass of the film. Nevertheless, as the time passes, degradation of the film is inevitable and, with the reduction of the polymeric chains' integrity, those interactions are also lost. In the presence of elastase, films degradation appeared to be minimized as the content of CA increased in the blend. Even though CA is chemically simple, its structure is complex, and often requires the action of various enzymatic complexes to ensure complete degradation of the material.[52] Because of the intermolecular bond generated between the polymers' hydroxyl groups, the enzymatic stability of the film increased becoming less vulnerable to the action of elastase. In physiological serum, films' degradation increased with time, with more than 20% of the films' mass being lost after 28 days of incubation. These results show that storage of the PVA/CA films is possible at 37 ºC without much loss of polymeric integrity. Storage of the PVA/CA films in physiological serum was also tested for 28 days at 4 ºC, registering a maximum of ≈ 4 % of mass loss for all tested blends (data not shown). Finally, it is important to refer that after only one day of incubation, most films experienced mass reduction. This is an important feature for wound-healing applications, since with the

degradation of the film in the first 24 h of contact with the wounded bed (physiological media), biomolecules or antimicrobial agents entrapped within the polymeric matrix can also be release, allowing for a phased topical and transdermal delivery.

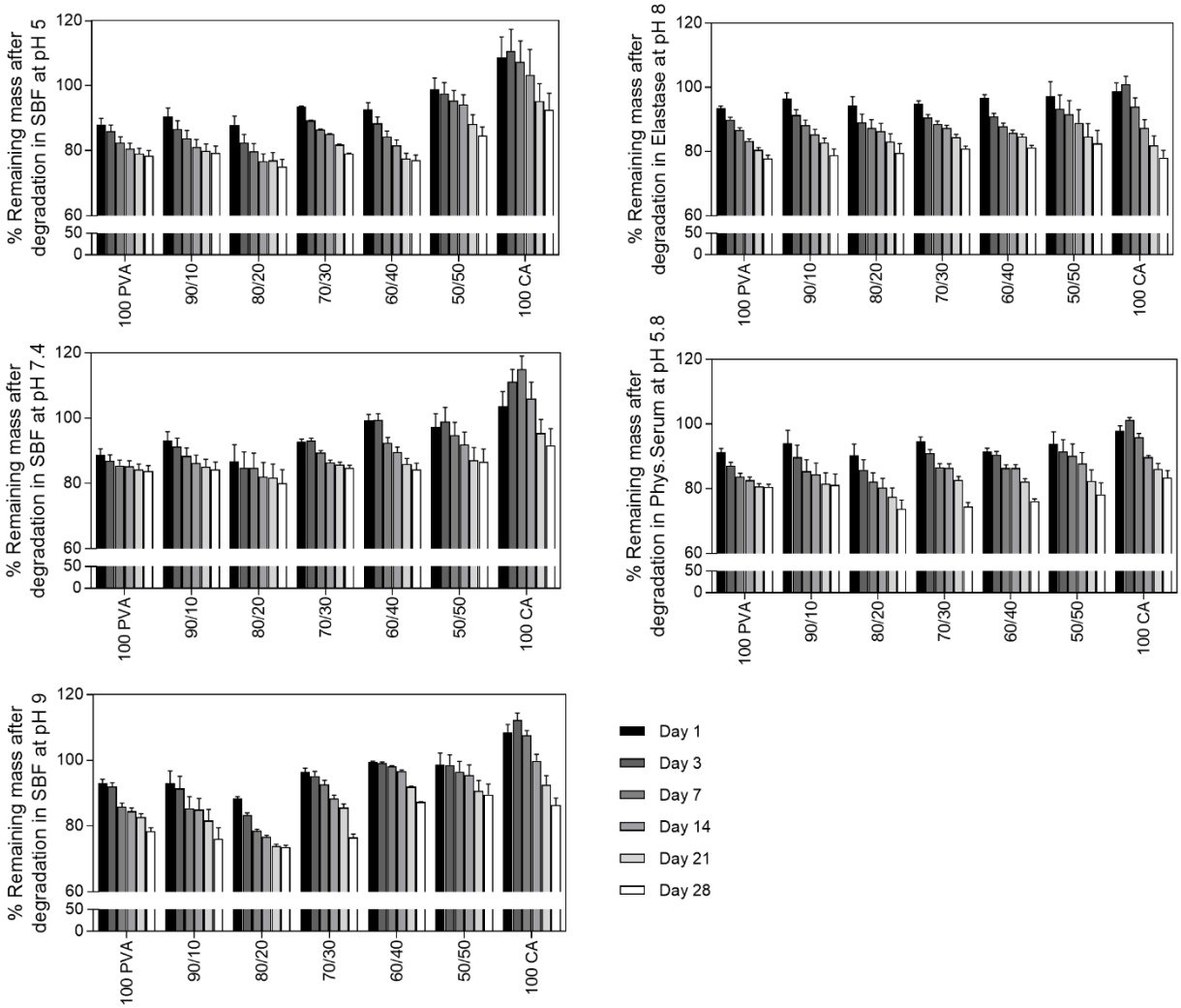

Figure 5. PVA/CA films degradation profile in SBF at pH 5, 7.4 and 9, elastase buffer at pH 8 and commercial physiological serum at pH 5.8, from 1 to 28 days at 37 ºC.

3.6 Antimicrobial Activity. The antimicrobial efficacy of the PVA/CA films was tested against *S. aureus*, *S. epidermidis* and *E. coli* bacteria (control data on the bacteria viability after 24 h culture in PBS can be found in Figure S1 in Supporting Information). Bare films and films functionalized with vancomycin and LL37, via dopamine, were tested. The amount of LL37 present on the surface of the PVA/CA films was determined at

21.6 ± 2.5 μg/cm^2 through amino groups detection using Sulfo-SDTB test, a value significantly higher than the ≈ 4.6 μg/cm^2 obtained without pDOPA. Since vancomycin is a large molecule (glycopeptide with a molecular weight of 1449.3 g/mol) formed by more than one amino group, the amount detected on the PVA/CA surfaces was superior to LL37, reaching the 32.8 ± 3.1 μg/cm^2. In any case, the successful binding of the biomolecules was confirmed. The contributions of vancomycin and LL37 to the films surface properties (functional groups, thermal stability, tensile strength, porosity, swelling and degradation) did not induce any significant differences from the data presented in the previous sections and as such were neglected.

Prior to determining the antimicrobial efficacy of the functionalized polymeric films, the antimicrobial agents were tested in suspension (free state) against the three microorganisms to confirm their efficiency against the selected strains. Data from Table 3 revealed the efficacy of vancomycin and LL37 against the three kinds bacteria, with a reduction of more than 90% of the microorganisms. It was also seen that both biomolecules were most effective against the *S. epidermidis* bacteria. While functionalized (Figure 6A), surfaces treated with LL37 demonstrated the highest antibacterial efficacy from the group: ≈ 75% for *S. aureus*, ≈ 85% for *S. epidermidis* and ≈ 60% for *E. coli*. LL37 is effective against a broad spectrum of bacteria that include both Gram-positive and Gram-negative. *In vitro* assays, using lipid bilayers, have shown that LL37 permeabilizes bacteria membranes by a carpeting (non-pore) or toroidal (pore) mechanism, ultimately leading to loss of membrane integrity and cell apoptosis.[53] Under dynamic conditions, the antimicrobial action may occur by contact or by leaching of the antimicrobial molecules. Here, however, it is not possible to determine with certainty if only one or both mechanisms are taking place. Still, assuming the potential bactericidal mechanisms of the helical AMP LL37 is its interaction with the bacterial membrane, lateral mobility of the peptide molecules is required.[20] Since biding via dopamine is independent of peptide conformation and is based on the principle of physisorption, it is likely the AMPs to be capable of detaching from the film and penetrating the bacteria membrane or to adopt a different orientation, suggesting some degree of freedom. The vancomycin ability to inhibit bacteria action was inferior to that of the LL37, putting in evidence the superior antimicrobial performance of AMPs compared to antibiotics, even at smaller concentrations (21.6 ± 2.5 μg/cm^2 LL37 vs 32.8 ± 3.1 μg/cm^2 vancomycin). The bacterial inhibition of vancomycin functionalized surfaces was about 55%, 65% and 50% for *S. aureus*, *S. epidermidis* and *E. coli*, respectively. Even though vancomycin was not capable of inhibiting bacterial action completely, reports have shown that this may

actually hinder biofilm formation.[54] In all studies, the antibacterial activity was more important against Gram-positive (*S. aureus* and *S. epidermidis*) than Gram-negative (*E. coli*) bacteria. The cell wall of Gram-positive bacteria is composed of a thick peptidoglycan layer formed of linear polysaccharide chains cross-linked by short peptides, resulting in a 3D rigid structure, while the cell wall of Gram-negative bacteria is more structurally and chemically complex with a thin peptidoglycan layer adjacent to the cytoplasmic membrane and a lipopolysaccharidic outer membrane, which hydrophilic nature and the presence of periplasmic-space enzymes are capable of degrading molecules introduced from the outside.[55, 56]

The influence of the adsorption of albumin on the films antimicrobial properties was noticeable against all three bacteria (Figure 6B). An important reduction on the functionalized films antimicrobial efficacy was registered (between 20 and 30% for all surfaces). Albumin has shown obvious inhibitory effects against many bacteria, preventing their binding to polymeric, ceramic and metal surfaces.[57] However, its effect is mostly in preventing bacterial adhesion rather than killing bacteria. In fact, in contact with the vancomycin and LL37 functionalized films, BSA may bind with these molecules, reducing the free fraction of the antimicrobial agent available for bacterial killing, since only the non-protein bound portion will be active to interact with the microorganism. BSA is endowed with many specific and non-specific binding sites accessible to proteins/peptides and drugs, which bind via electrostatic and dipolar forces, hence compromising their antimicrobial activity.[58]

Overall, no significant differences were observed amongst polymeric blends regardless of the presence of immobilized antimicrobial agents. The control samples displayed antibacterial activity against all pathogens. This happens because bacteria can get entrapped within the polymeric matrix via their pores, decreasing the number of colonies in solution.

Table 3. LL37 and vancomycin antimicrobial efficacy against *S. aureus*, *S. epidermidis* and *E. coli* bacteria (% of growth inhibition ± SD and log_{10}). Antimicrobial agents suspended in solution, not functionalized.

Antimicrobial Agents	***S. aureus***		***S. epidermidis***		***E. coli***	
	Reduction (% ± SD)	**Log_{10}**	**Reduction (% ± SD)**	**Log_{10}**	**Reduction (% ± SD)**	**Log_{10}**
LL37	99.69 ± 0.14	2.51	99.94 ± 0.04	3.24	97.46 ± 0.50	1.59

Vancomycin	97.93 ± 0.65	1.68	98.20 ± 0.45	1.74	94.75 ± 1.14	1.28

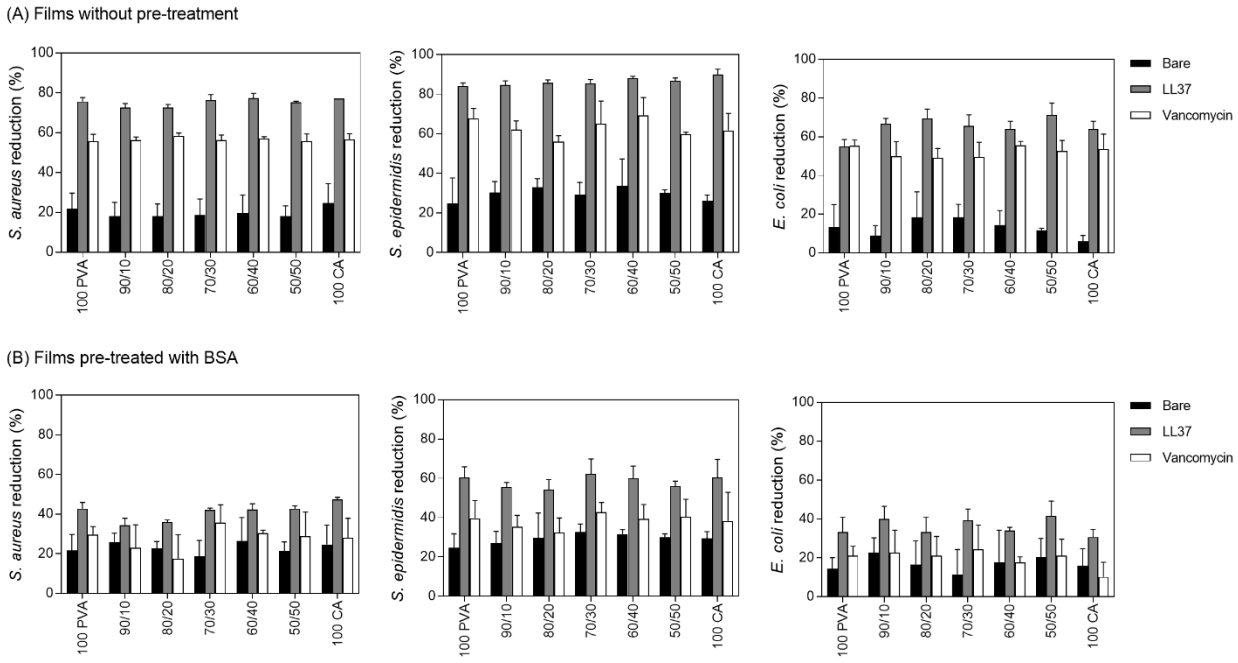

Figure 6. Antimicrobial action of PVA/CA films bare (control) and functionalized with LL37 and vancomycin. The *S. aureus*, *S. epidermidis* and *E. coli* growth inhibition (%) were analyzed in the (A) absence and (B) presence of BSA (adsorption at 4 mg/mL for 1 h) surface pre-treatment.

3.7 Clotting Time. The coagulation cascade consists of three pathways, the contact activation (intrinsic), the tissue factor (extrinsic), and the final common pathway of factor X, thrombin, and fibrin. In physiological media, particularly in contact with blood, biomaterials are quickly surrounded by proteins that instantly adsorb onto the surface and activate a cascade of reactions that ultimately lead to the formation of a blood clot.[59] Depending on the surface properties of these biomaterials the coagulation cascade and, consequently, the time necessary to induce clotting may be altered. Here, the clotting times of recalcified plasma were evaluated in the presence of bare (control), and LL37 and vancomycin modified films (Figure 7). In this assay, recalcified plasma was allowed to clot in contact with a film under dynamic conditions, and coagulation was triggered through the intrinsic pathway, in which contact activation of Factor XII, high-molecular-weight kininogen and prekallikrein occurs. The addition of Ca^{2+} (Factor IV) to anticoagulated human plasma activates prothrombin (Factor II), converting it into thrombin, which then cleaves fibrinogen leading to insoluble fibrin, the

framework of the thrombus.[31] TCPS was used as negative control, while glass was used as positive control. Data determined TCPS as the least thrombogenic material (≈ 25 min) and glass the most (≈ 4 min), inducing the quickest clotting time from all samples. These results are consistent with previous findings.[30, 31, 60, 61] It should be noted, however, that all results may have been influenced at some degree by TCPS, since some lateral space of the wells, where the samples were placed, was still exposed to the plasma solution. Films without any surface treatment took less time than TCPS to induce clotting (≈ 21 min). As no differences were detected between PVA/CA ratios, these results reflect both PVA and CA alone and the polymeric blends. Previous reports on the clotting time of PVA and bacterial cellulose have also shown the absence of statistical differences between blends and single polymers.[61] The presence of porosity and, consequently, the larger surface area of the PVA/CA films compared to TCPS increased the contact with the recalcified plasma, allowing for a quicker clotting time. Surfaces treated with vancomycin behave similarly to the bare films, meaning this antibiotic has little effect on the coagulation process. Contrary, films treated with the AMP LL37 displayed a unique performance, revealing a short clotting time (≈ 10 min) and demonstrating great capacity to activate the intrinsic coagulation cascade. It is likely that the plasma proteins Factor XII, high-molecular-weight kininogen and prekallikrein to have preferentially adsorbed onto these surfaces, attracted by the presence of this AMP, leading to a faster contact activation of the coagulation process. As seen earlier, LL37 is a powerful antimicrobial peptide; however, it also regulates the innate immune response, intervening in different phases of the healing process.[6, 15, 17, 18] In an open wound, the LL37 contained within the granules of platelets is released to the local environment to support microbial clearance, activate the inflammatory response and modulate thrombosis and hemostasis. Reports have shown LL37 to promote thrombus formation, reduce the clotting time (in mice tails) and, generally, accelerate healing.[15, 62] The mechanisms by which LL37 intervenes in the coagulation cascade are still under investigation; however, it is clear that its presence within neutrophils, monocytes and platelets to be extremely important during this process.

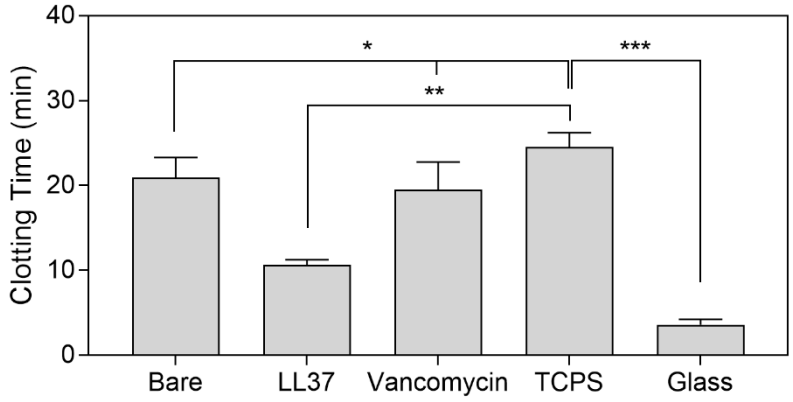

Figure 7. Clotting time of recalcified plasma in the presence of PVA/CA films bare (control) and functionalized with LL37 and vancomycin. TCPS and glass were used as negative and positive controls, respectively. No significant differences were visually perceived between PVA/CA ratios. Therefore, only the average between surface treatments was provided. Statistical significance between the surfaces and TCPS is indicated by * (*$p<0.05$, **$p<0.001$, ***$p<0.0001$, One-Way ANOVA following Tukey's Posttest).

4. Conclusions

PVA/CA films, at different ratios, were successfully produced via a combination of solvent casting and phase inversion. Presence of the two polymers within the blends was confirmed and a small improvement in the blended films thermodynamic behavior was registered, compared to the single polymer films. The mechanical resistance of the films became compromised with the increased content of CA within the blends, which also instigated pores formation. The hydration capacity of the films was independent of polymeric blend putting in evidence important interactions between polymers and between polymeric chains and water molecules. All films experienced a mass loss of ≈ 20% after 28 days of incubation in different physiological media. The most acidic solution (SBF at pH 5) registered a superior mass loss due to the increased formation of OH^- and H^+ radicals that participate in oxidation reactions of the polymer macroradicals and, thereby, making chemical effects dominant in the degradation of the PVA/CA films.

The films antimicrobial action against *S. aureus*, *S. epidermidis* and *E. coli* was significantly enhanced by the addition of LL37; however, it was independent of polymeric ratio. LL37 results were significantly superior to those obtained with vancomycin, putting in evidence the superior antimicrobial performance of AMPs over

antibiotics against both Gram-positive and Gram-negative bacteria. Presence of albumin reduced bacteria inhibition in all tested groups, most likely due to the binding of the protein molecules to the antimicrobial agents, reducing the free fraction available for bacterial killing. Films treated with the AMP LL37 accelerated clotting time (≈ 10 min) above vancomycin and bare surfaces, demonstrating great capacity to activate the intrinsic coagulation cascade. In the end, the potential of LL37 functionalized PVA/CA films for prospective wound-healing applications was demonstrated.

Acknowledgements

Authors acknowledge the Portuguese Foundation for Science and Technology (FCT), FEDER funds by means of Portugal 2020 Competitive Factors Operational Program (POCI) and the Portuguese Government (OE) for funding the project PEPTEX with reference POCI-01-0145-FEDER-028074. Authors also acknowledge project UID/CTM/00264/2019 of Centre for Textile Science and Technology (2C2T), funded by national funds through FCT/MCTES.

Conflicts of Interest

There are no conflicts of interest to declare.

References

1. Frykberg, R.G.;Banks, J. *Adv. Wound Care* **2015**, 4, 560.
2. Dreifke, M.B.;Jayasuriya, A.A.;Jayasuriya, A.C. *Materials Science and Engineering: C* **2015**, 48, 651.
3. Schönfelder, U.;Abel, M.;Wiegand, C.;Klemm, D.;Elsner, P.;Hipler, U.-C. *Biomaterials* **2005**, 26, 6664.
4. Schiffer, D.;Blokhuis- Arkes, M.;van der Palen, J.;Sigl, E.;Heinzle, A.;Guebitz, G. *Br. J. Dermatol.* **2015**, 173, 1529.
5. Langemo, D.K. *Advances in Skin & Wound Care* **1991**, 4, 14.
6. Felgueiras, H.P.;Amorim, M.T.P. *Colloids Surf. B Biointerfaces* **2017**, 156, 133.
7. Eming, S.A.;Martin, P.;Tomic-Canic, M. *Science translational medicine* **2014**, 6, 265sr6.
8. Kataria, K.;Gupta, A.;Rath, G.;Mathur, R.;Dhakate, S. *International journal of pharmaceutics* **2014**, 469, 102.
9. Felgueiras, H.P.;Amorim, M. in IOP Conf. Ser. Mater. Sci. Eng.: 2017; IOP Publishing.
10. Sweeney, I.R.;Miraftab, M.;Collyer, G. *International wound journal* **2012**, 9, 601.
11. Halstead, F.D.;Rauf, M.;Bamford, A.;Wearn, C.M.;Bishop, J.R.;Burt, R.;Fraise, A.P.;Moiemen, N.S.;Oppenheim, B.A.;Webber, M.A. *Burns* **2015**, 41, 1683.
12. Gottrup, F.;Apelqvist, J.;Bjarnsholt, T.;Cooper, R.;Moore, Z.;Peters, E.J.;Probst, S. *Journal of wound care* **2014**, 23, 477.

13. Turner, J.;Cho, Y.;Dinh, N.-N.;Waring, A.J.;Lehrer, R.I. *Antimicrob. Agents Chemother.* **1998**, 42, 2206.
14. Scott, M.G.;Davidson, D.J.;Gold, M.R.;Bowdish, D.;Hancock, R.E. *J. Immunol.* **2002**, 169, 3883.
15. Ramos, R.;Silva, J.P.;Rodrigues, A.C.;Costa, R.;Guardão, L.;Schmitt, F.;Soares, R.;Vilanova, M.;Domingues, L.;Gama, M. *Peptides* **2011**, 32, 1469.
16. Chereddy, K.K.;Her, C.-H.;Comune, M.;Moia, C.;Lopes, A.;Porporato, P.E.;Vanacker, J.;Lam, M.C.;Steinstraesser, L.;Sonveaux, P. *J. Control. Release* **2014**, 194, 138.
17. Sørensen, O.E.;Follin, P.;Johnsen, A.H.;Calafat, J.;Tjabringa, G.S.;Hiemstra, P.S.;Borregaard, N. *Blood* **2001**, 97, 3951.
18. Koczulla, R.;Von Degenfeld, G.;Kupatt, C.;Krötz, F.;Zahler, S.;Gloe, T.;Issbrücker, K.;Unterberger, P.;Zaiou, M.;Lebherz, C. *J. Clin. Invest.* **2003**, 111, 1665.
19. Grönberg, A.;Mahlapuu, M.;Ståhle, M.;Whately- Smith, C.;Rollman, O. *Wound Repair Regen.* **2014**, 22, 613.
20. Gabriel, M.;Nazmi, K.;Veerman, E.C.;Nieuw Amerongen, A.V.;Zentner, A. *Bioconjug. Chem.* **2006**, 17, 548.
21. Gatti, J.W.;Smithgall, M.C.;Paranjape, S.M.;Rolfes, R.J.;Paranjape, M. *Biomed. Microdevices* **2013**, 15, 887.
22. Fumakia, M.;Ho, E.A. *Mol. Pharm.* **2016**, 13, 2318.
23. Chouhan, D.;Janani, G.;Chakraborty, B.;Nandi, S.K.;Mandal, B.B. *J. Tissue Eng. Regen. Med.* **2018**, 12, e1559.
24. Koski, A.;Yim, K.;Shivkumar, S. *Materials Letters* **2004**, 58, 493.
25. Czaja, W.;Krystynowicz, A.;Bielecki, S.;Brown, R.M. *Biomaterials* **2006**, 27, 145.
26. Yin, J.;Fan, H.;Zhou, J. *Desalin. Water Treat.* **2016**, 57, 10572.
27. Felgueiras, H.P.;Wang, L.;Ren, K.;Querido, M.;Jin, Q.;Barbosa, M.;Ji, J.;Martins, M. *ACS Appl. Mater. Interfaces* **2017**, 9, 7979.
28. Ahmad, A.;Yusuf, N.;Ooi, B. *Desalin.* **2012**, 287, 35.
29. Edwards, J.V.;Howley, P.;Cohen, I.K. *Int. J. Pharm.* **2004**, 284, 1.
30. Cao, L.;Chang, M.;Lee, C.Y.;Castner, D.G.;Sukavaneshvar, S.;Ratner, B.D.;Horbett, T.A. *J. Biomed. Mater. Res. A* **2007**, 81, 827.
31. Gonçalves, I.C.;Martins, M.C.L.;Barbosa, M.A.;Ratner, B.D. *Biomaterials* **2009**, 30, 5541.
32. Toprak, C.;Agar, J.N.;Falk, M. *J. Chem. Soc. Faraday Trans. 2* **1979**, 75, 803.
33. Wang, R.;Wang, Q.;Li, L. *Polym. Int.* **2003**, 52, 1820.
34. Sudiarti, T.;Wahyuningrum, D.;Bundjali, B.;Arcana, I.M. in IOP Conf. Ser. Mater. Sci. Eng.: 2017; IOP Publishing.
35. Zhang, L.-Z.;Wang, Y.-Y.;Wang, C.-L.;Xiang, H. *J. Membr. Sci.* **2008**, 308, 198.
36. Dias, C.R.;Rosa, M.J.;de Pinho, M.N. *J. Membr. Sci.* **1998**, 138, 259.
37. Guzman-Puyol, S.;Ceseracciu, L.;Heredia-Guerrero, J.A.;Anyfantis, G.C.;Cingolani, R.;Athanassiou, A.;Bayer, I.S. *Chem. Eng. J.* **2015**, 277, 242.
38. Lee, J.;Lee, K.J.;Jang, J. *Polym. Test.* **2008**, 27, 360.
39. Upadhyay, D.;Bhat, N. *J. Membr. Sci.* **2005**, 255, 181.
40. Kee, C.M.;Idris, A. *Sep. Purif. Technol.* **2010**, 75, 102.
41. Yavuz, G.;Felgueiras, H.P.;Ribeiro, A.I.;Seventekin, N.;Zille, A.;Souto, A.P. *ACS Applied Materials & Interfaces* **2018**,
42. Coelho, D.;Sampaio, A.;Silva, C.J.;Felgueiras, H.P.;Amorim, M.T.P.;Zille, A. *ACS Appl. Mater. Interfaces* **2017**, 9, 33107.
43. Qiu, K.;Netravali, A.N. *J. Mater. Sci.* **2012**, 47, 6066.
44. Qiu, K.;Netravali, A.N. *Composites Sci. Technol.* **2012**, 72, 1588.
45. El-Hefian, E.A.;Nasef, M.M.;Yahaya, A.H. *Journal of Chemistry* **2011**, 8, 91.
46. da Silva Meireles, C.;Rodrigues Filho, G.;Ferreira Jr, M.F.;Cerqueira, D.A.;Assunção, R.M.N.;Ribeiro, E.A.M.;Poletto, P.;Zeni, M. *Carbohydr. Polym.* **2010**, 80, 954.
47. Bernal-Ballén, A.;Kuritka, I.;Saha, P. *Int. J. Polym. Sci.* **2016**, 2016,
48. Alhosseini, S.N.;Moztarzadeh, F.;Mozafari, M.;Asgari, S.;Dodel, M.;Samadikuchaksaraei, A.;Kargozar, S.;Jalali, N. *Int. J. Nanomedicine* **2012**, 7, 25.
49. Young, C.-D.;Wu, J.-R.;Tsou, T.-L. *J. Membr. Sci.* **1998**, 146, 83.
50. Li, J.;Jiang, G.;Ding, F. *J. Appl. Polym. Sci.* **2008**, 109, 475.

51. Lin, C.-C.;Lee, L.-T.;Hsu, L.-J. *Int. J. Environ. Sci. Technol.* **2014**, 11, 831.
52. Calil, M.;Gaboardi, F.;Bardi, M.;Rezende, M.;Rosa, D. *Polym. Test.* **2007**, 26, 257.
53. Sochacki, K.A.;Barns, K.J.;Bucki, R.;Weisshaar, J.C. *Proc. Natl. Acad. Sci.* **2011**, 108, E77.
54. García-Vargas, M.;González-Chomón, C.;Magariños, B.;Concheiro, A.;Alvarez-Lorenzo, C.;Bucio, E. *Int. J. Pharm.* **2014**, 461, 286.
55. Malanovic, N.;Lohner, K. *Biochim. Biophys. Acta Biomembr.* **2016**, 1858, 936.
56. Schwechheimer, C.;Kuehn, M.J. *Nat. Rev. Microbiol.* **2015**, 13, 605.
57. Katsikogianni, M.;Missirlis, Y. *Eur. Cell Mater.* **2004**, 8, 37.
58. Sudlow, G.;Birkett, D.;Wade, D. *Mol. Pharmacol.* **1976**, 12, 1052.
59. Gorbet, M.B.;Sefton, M.V., in The Biomaterials: Silver Jubilee Compendium; Elsevier**2004**; p. 219.
60. Zhang, Z.;Zhang, M.;Chen, S.;Horbett, T.A.;Ratner, B.D.;Jiang, S. *Biomaterials* **2008**, 29, 4285.
61. Leitão, A.F.;Gupta, S.;Silva, J.P.;Reviakine, I.;Gama, M. *Colloids Surf. B Biointerfaces* **2013**, 111, 493.
62. Salamah, M.F.;Ravishankar, D.;Kodji, X.;Moraes, L.A.;Williams, H.F.;Vallance, T.M.;Albadawi, D.A.;Vaiyapuri, R.;Watson, K.;Gibbins, J.M. *Blood Adv.* **2018**, 2, 2973.

Graphical Abstract